

**Anion Binding Induced Conformational Changes Exploited for Recognition,
Sensing and Pseudorotaxane Disassembly**

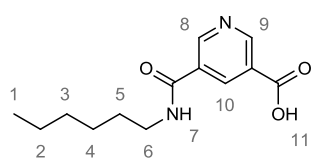
Graeme T. Spence, Carmen Chan, Fridrich Szemes and Paul D. Beer*

Department of Chemistry, University of Oxford,
Mansfield Road, Oxford, OX1 3TA, UK.

Supplementary Information

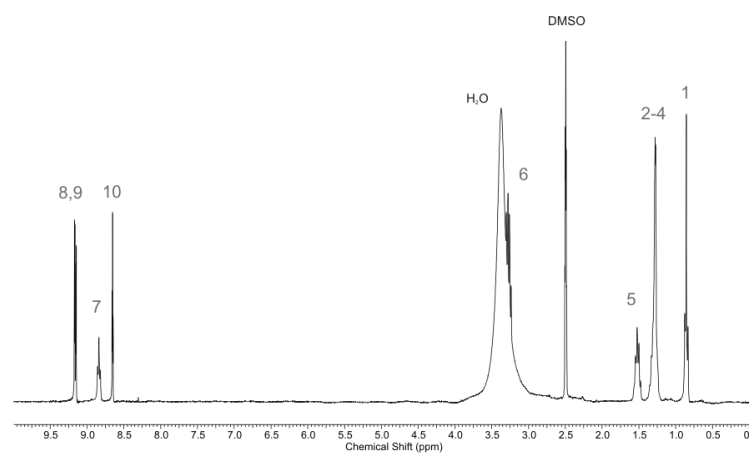
Part I: Spectral Characterisation of Novel Compounds	S2
Part II: ¹H-¹H 2D ROESY NMR Spectrum	S14
Part III: ¹H NMR Titrations	S15
Protocols	S15
Example Titration Spectra	S16
Binding Curves	S17
Part IV: Fluorescence and UV/Vis Studies	S20
Fluorescence Spectrum	S20
Fluorescence Protocol	S20
UV/Vis Protocol	S20
Binding Curves	S21
UV/Vis and Excitation Spectra	S22
Part V: References	S22

Compound 3

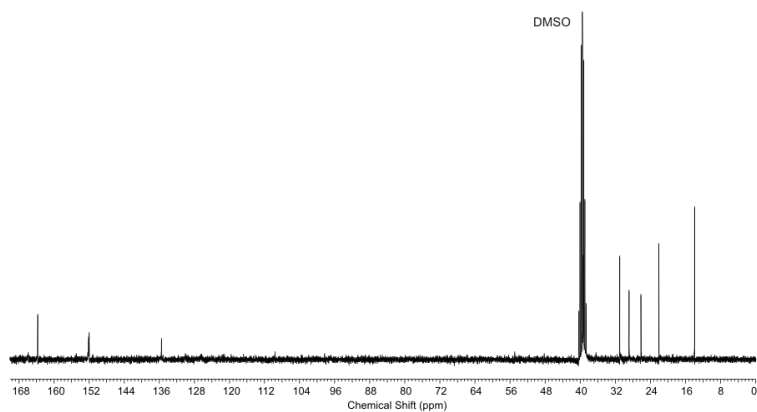


3

¹H NMR (300 MHz, *d*⁶-DMSO)



¹³C NMR (75.5 MHz, *d*⁶-DMSO)

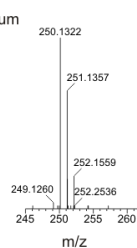


HR (FI +ve) MS

Isotope Model

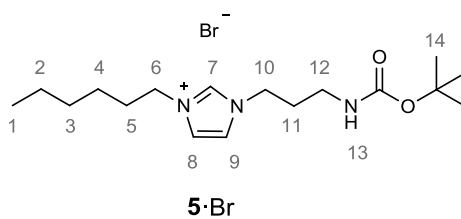


Actual Spectrum

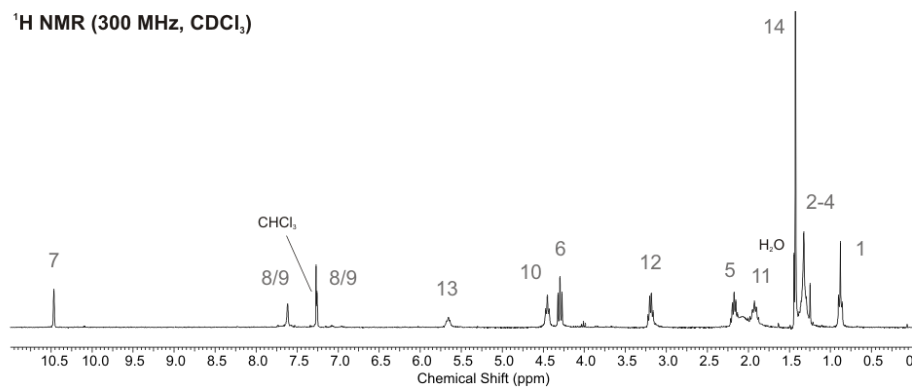


Supplementary Fig. S2 ¹H and ¹³C NMR spectra and high resolution MS of compound 3.

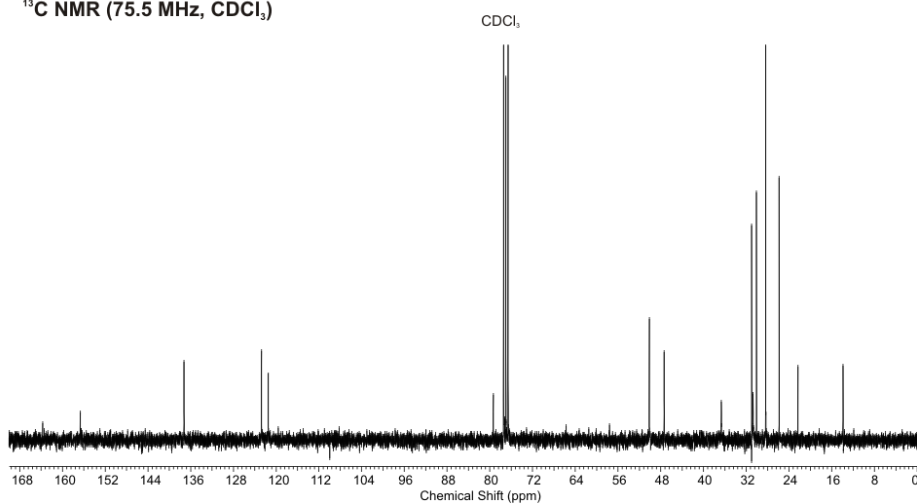
Compound 5·Br



¹H NMR (300 MHz, CDCl₃)

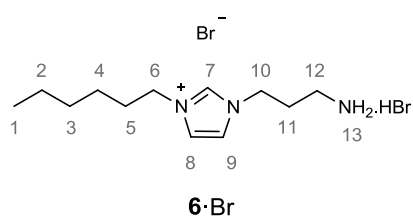


¹³C NMR (75.5 MHz, CDCl₃)

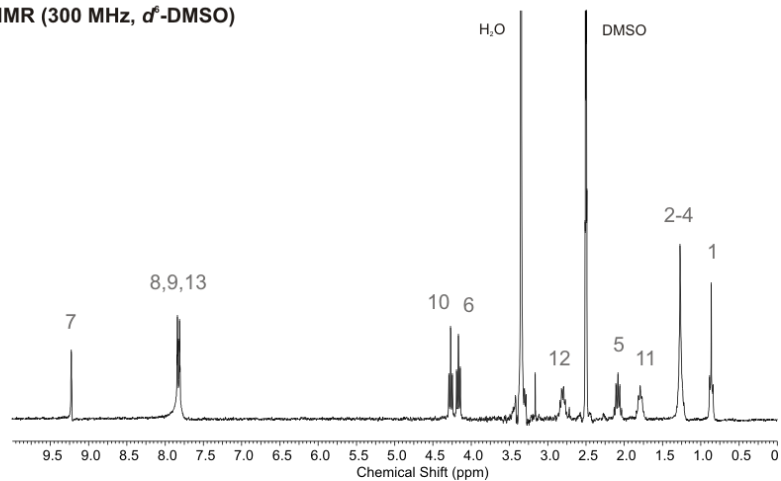


Supplementary Fig. S3 ¹H and ¹³C NMR spectra of compound 5·Br.

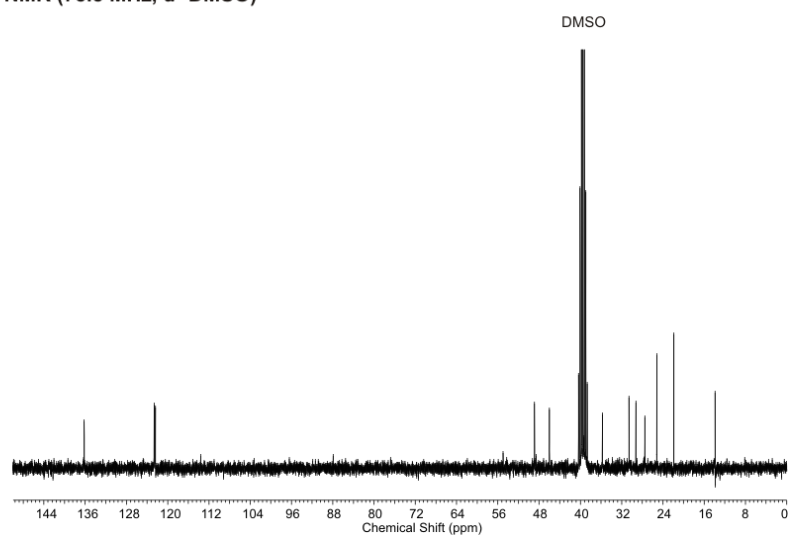
Compound **6**·Br



¹H NMR (300 MHz, *d*⁶-DMSO)

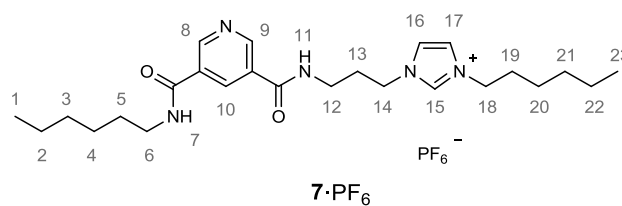


¹³C NMR (75.5 MHz, *d*⁶-DMSO)

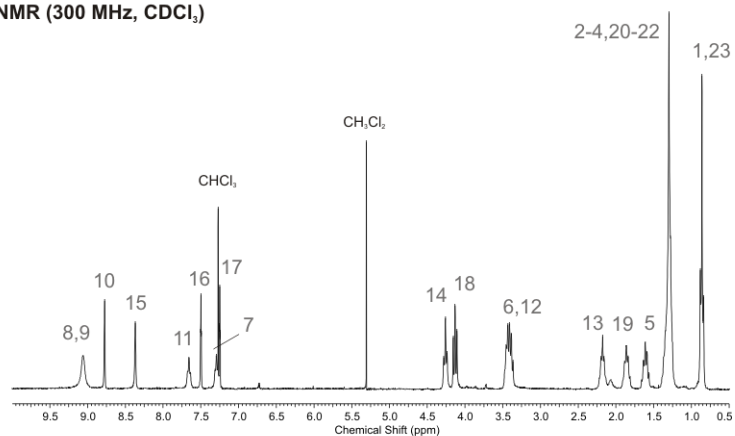


Supplementary Fig. S4 ¹H and ¹³C NMR spectra of compound **6**·Br.

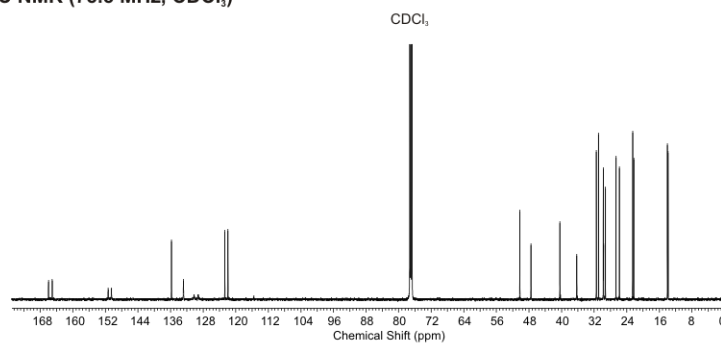
Receptor **7**·PF₆



¹H NMR (300 MHz, CDCl₃)

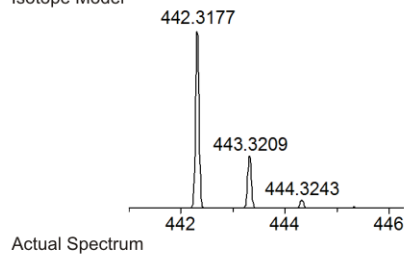


¹³C NMR (75.5 MHz, CDCl₃)

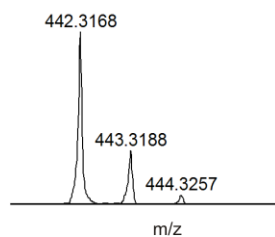


HR (ESI +ve) MS

Isotope Model

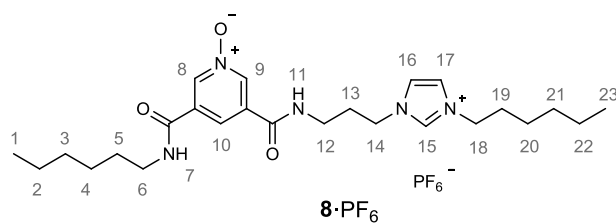


Actual Spectrum

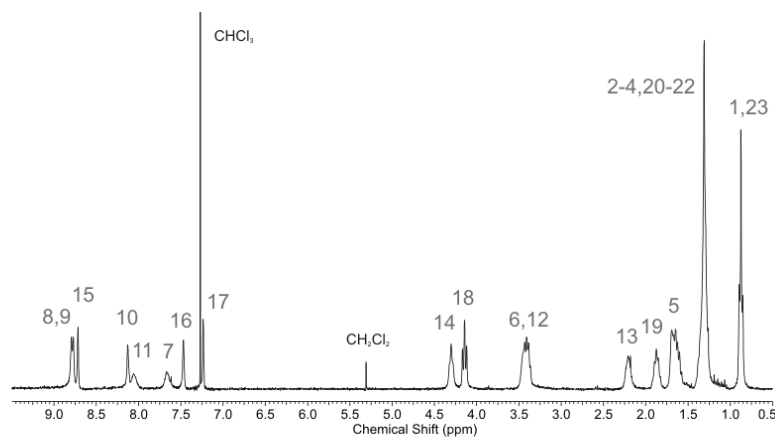


Supplementary Fig. S5 ¹H and ¹³C NMR spectra and high resolution MS of receptor **7**·PF₆.

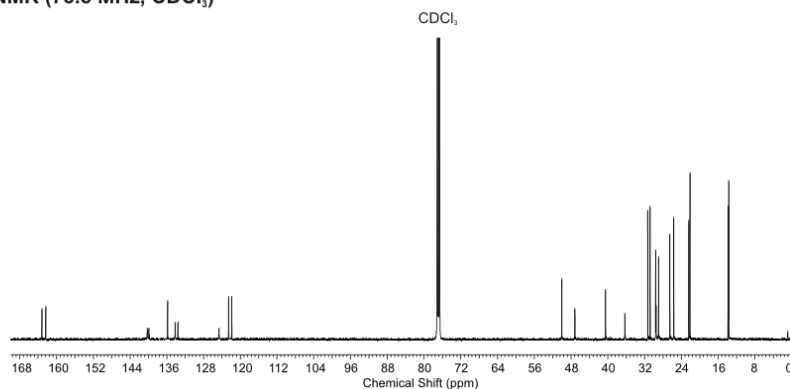
Receptor **8**·PF₆



¹H NMR (300 MHz, CDCl₃)

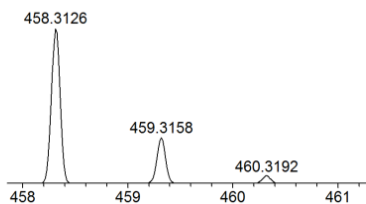


¹³C NMR (75.5 MHz, CDCl₃)

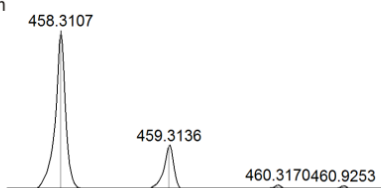


HR (ESI +ve) MS

Isotope Model



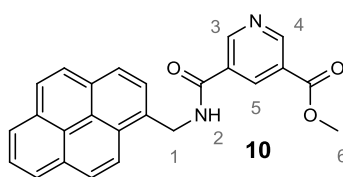
Actual Spectrum



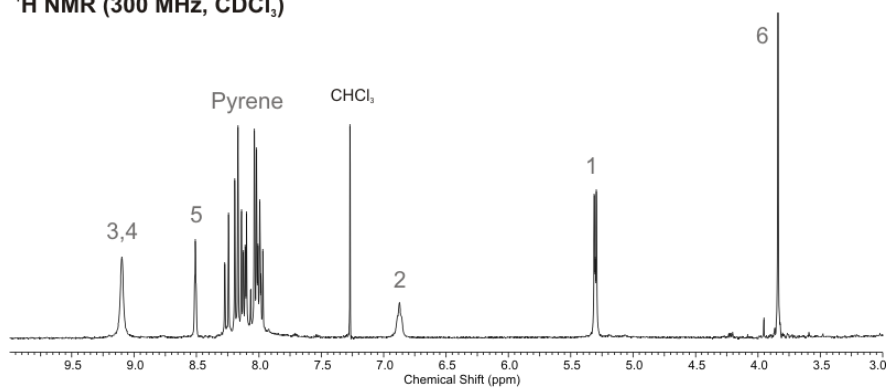
m/z

Supplementary Fig. S6 ¹H and ¹³C NMR spectra and high resolution MS of receptor **8**·PF₆.

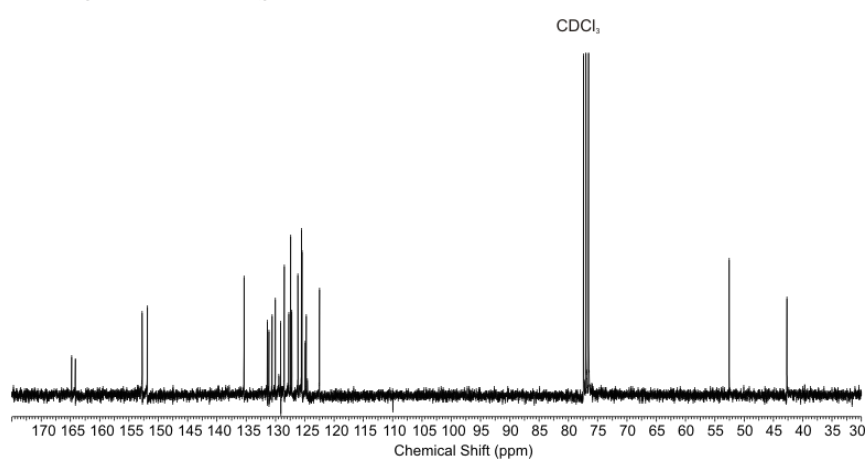
Compound **10**



¹H NMR (300 MHz, CDCl₃)

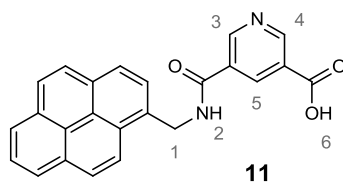


¹³C NMR (75.5 MHz, CDCl₃)

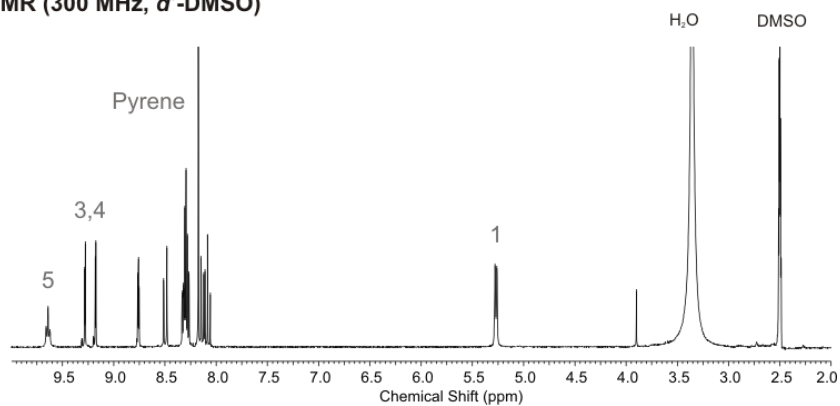


Supplementary Fig. S8 ¹H and ¹³C NMR spectra of compound **10**.

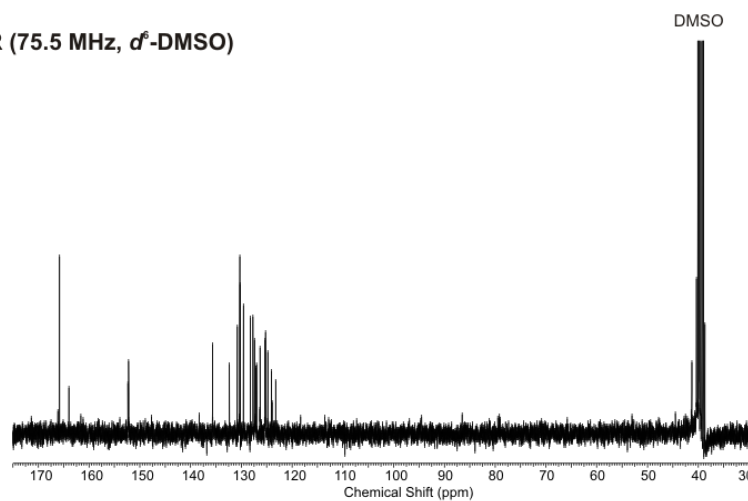
Compound 11



^1H NMR (300 MHz, d^6 -DMSO)

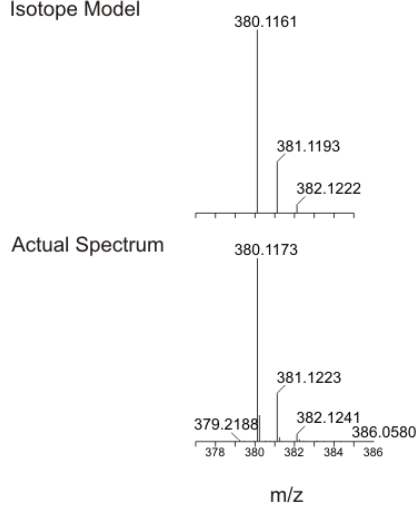


^{13}C NMR (75.5 MHz, d^6 -DMSO)



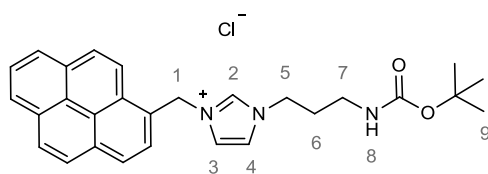
HR (FI +ve) MS

Isotope Model



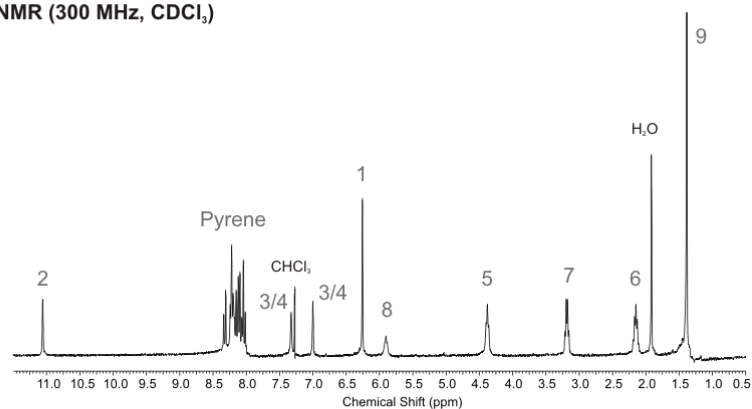
Supplementary Fig. S9 ^1H and ^{13}C NMR spectra and high resolution MS of compound 11.

Compound **12**·Cl

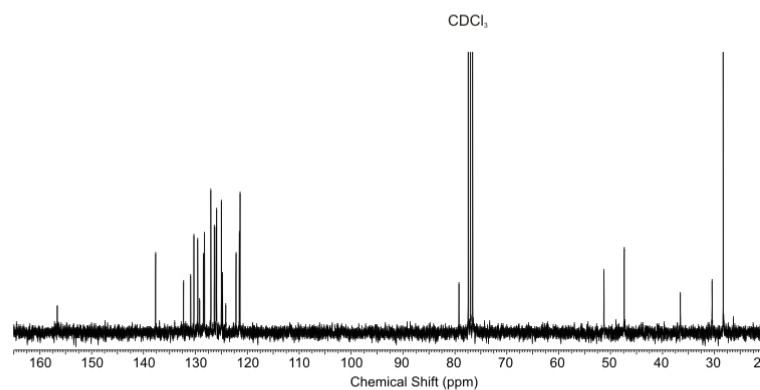


12·Cl

¹H NMR (300 MHz, CDCl₃)

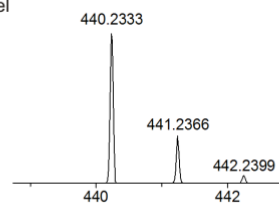


¹³C NMR (75.5 MHz, CDCl₃)

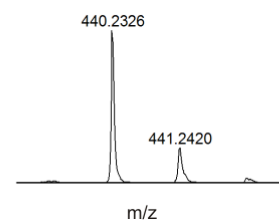


HR (ESI +ve) MS

Isotope Model

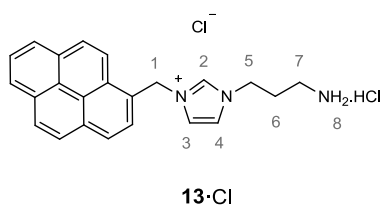


Actual Spectrum

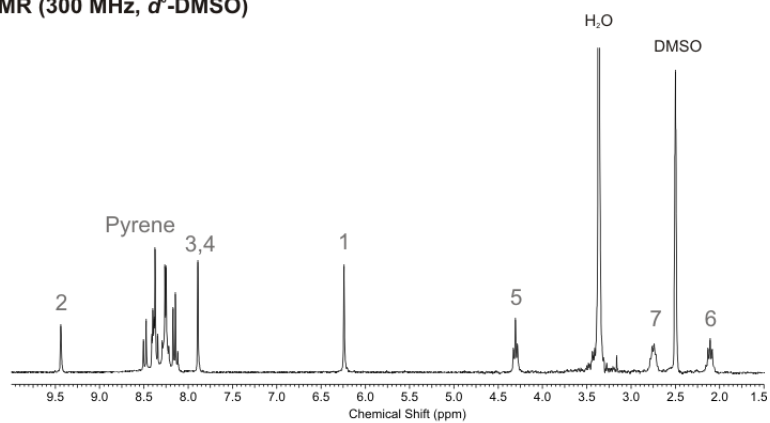


Supplementary Fig. S10 ¹H and ¹³C NMR spectra and high resolution MS of compound **12**·Cl.

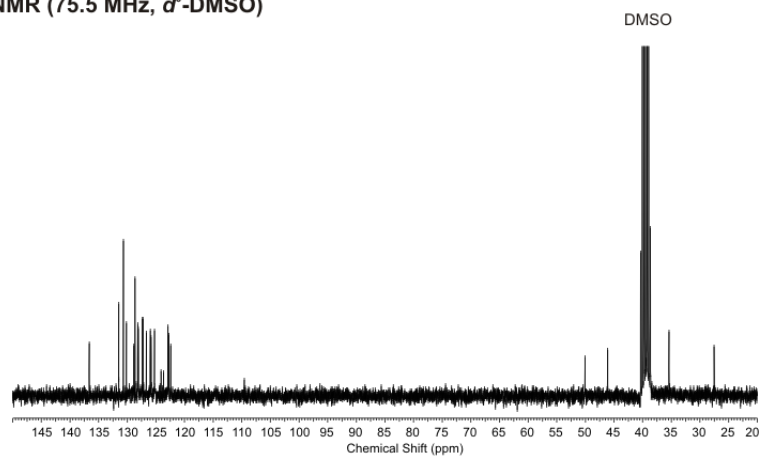
Compound **13**·Cl



¹H NMR (300 MHz, *d*⁶-DMSO)

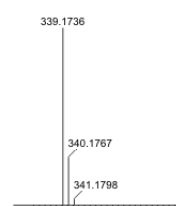


¹³C NMR (75.5 MHz, *d*⁶-DMSO)

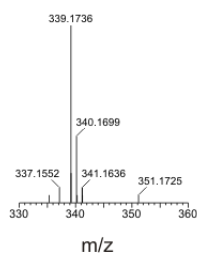


HR (FI +ve) MS

Isotope Model

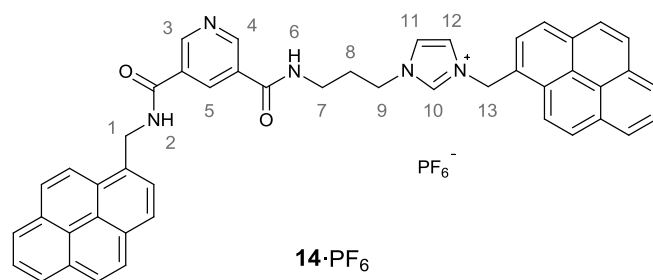


Actual Spectrum

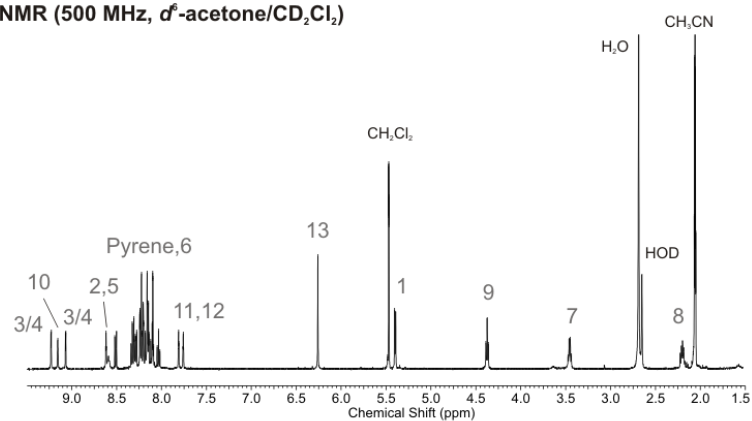


Supplementary Fig. S11 ¹H and ¹³C NMR spectra and high resolution MS of compound **13**·Cl.

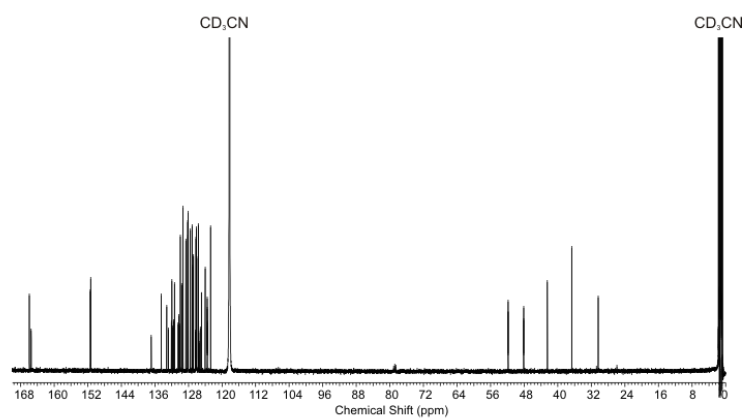
Receptor **14**·PF₆



¹H NMR (500 MHz, d⁶-acetone/CD₂Cl₂)

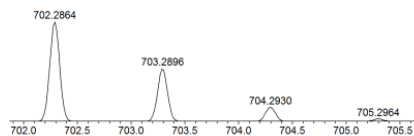


¹³C NMR (125.8 MHz, CD₃CN)

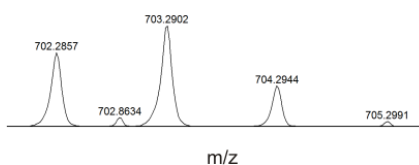


HR (ESI +ve) MS

Isotope Model



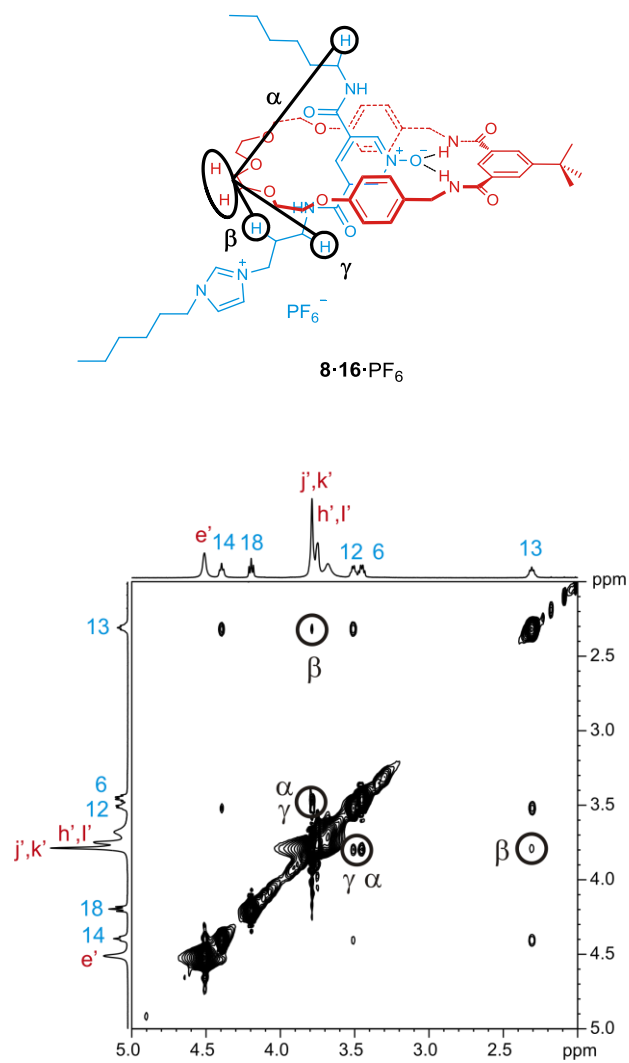
Actual Spectrum



Supplementary Fig. S12 ¹H and ¹³C NMR spectra and high resolution MS of receptor **14**·PF₆.

Part II: ^1H - ^1H 2D ROESY NMR Spectrum

Pseudorotaxane **8**·**16**· PF_6



Supplementary Fig. S13 Portion of the ^1H - ^1H ROESY spectrum of **8**·**16**· PF_6 (CDCl_3 , 500 MHz, 293 K). Intercomponent correlations are marked on the structure.

Part III: ^1H NMR Titrations

Protocols

All ^1H NMR titrations were conducted at 293 K with the spectra recorded on a Varian Unity Plus 500 spectrometer.

Receptors **7**·PF₆, **8**·PF₆ and **9**·(PF₆)₂:

To a 0.60 mL, 2.0×10^{-3} M solution of the host were added aliquots of the guest such that spectra were recorded at 0.2, 0.4, 0.6, 0.8, 1.0, 1.2, 1.4, 1.6, 1.8, 2.0, 2.5, 3.0, 4.0, 5.0, 7.0 and 10.0 equivalents, with a total of 100 μL added. The pyridine/pyridine N-oxide/pyridinium proton 10 was monitored throughout the titrations. The resultant curves were analysed as approximations of a Job-plot, and association constants obtained by WinEQNMR2 analysis.

Pseudorotaxane Titrations:

To a 0.60 mL, 2.0×10^{-3} M solution of the host macrocycle (**15** or **16**) were added aliquots of thread **8**·PF₆ such that spectra were recorded at 0.2, 0.4, 0.6, 0.8, 1.0, 1.2, 1.4, 1.6, 1.8, 2.0, 2.5, 3.0, 4.0, 5.0, 7.0 and 10.0 equivalents, with a total of 100 μL added. The macrocycle phenolic/hydroquinone protons (f or g'/h') were monitored throughout the titrations, and association constants were obtained by WinEQNMR2 analysis.

Pseudorotaxane Disassembly Titration:

To a 0.60 mL, 2.0×10^{-3} M solution of 1:1 macrocycle (**15** or **16**) and pyridine N-oxide thread **8**·PF₆ were added aliquots of TBACl such that spectra were recorded at 0.2, 0.4, 0.6, 0.8, 1.0, 1.2, 1.4, 1.6, 1.8, 2.0, 2.5, 3.0, 4.0, 5.0, 7.0 and 10.0 equivalents, with a total of 100 μL added.

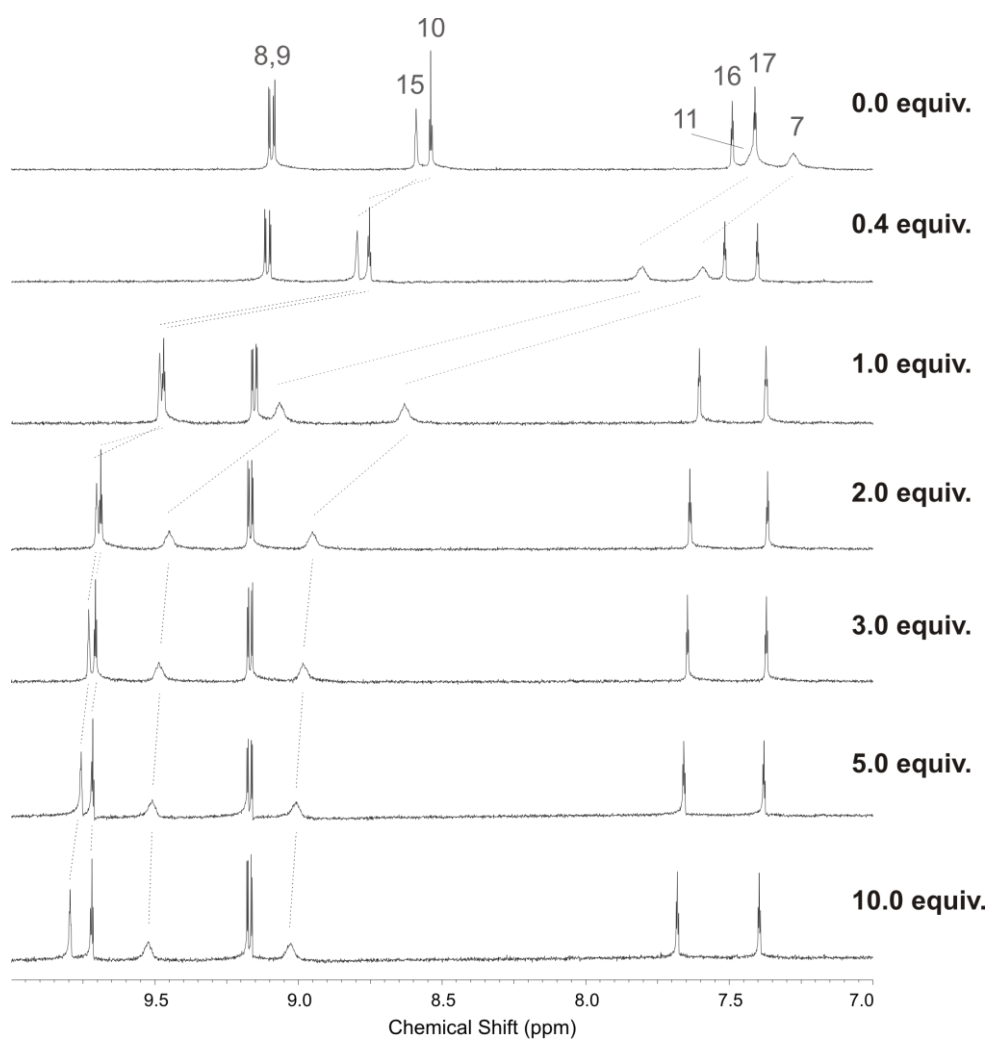
WinEQNMR2¹:

The titration data were analysed initially using approximations of Job plots to confirm the binding stoichiometries.²

Association constants were then obtained using WinEQNMR2¹ computer programme as the associations were found to be fast on the NMR timescale. The values of the observed chemical shift in the monitored proton signal and the species concentrations were entered for every titration point and estimates for the binding constant and limiting chemical shifts were made. The parameters were refined using non-linear least-squares analysis to obtain the best fit between observed and calculated chemical shifts for a 1:1 binding stoichiometry. The

program reveals the accuracy of the calculated binding isotherm, and the input parameters were varied until the best-fit values of the stability constants, and their errors, converged. For ease of comparison and to provide the best indication of the accuracy of the fit, the calculated association constants and their errors are given as absolute values without any rounding, e.g. 5731 (957) M^{-1} . As a consequence, the association constants are often quoted to significant figures beyond that of their error values, and this is taken into consideration when discussing binding trends.

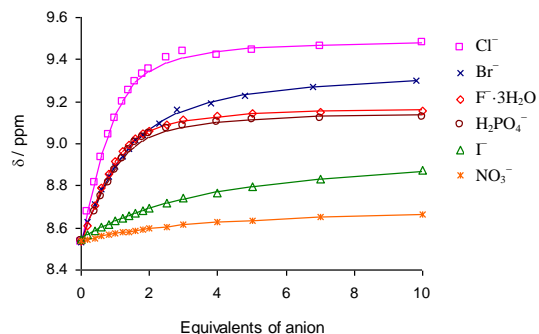
Example Titration Spectra



Supplementary Fig. S14 Partial 1H NMR spectra (500 MHz) in CD_3CN at 293 K of pyridine receptor $7 \cdot PF_6$ upon addition of TBACl.

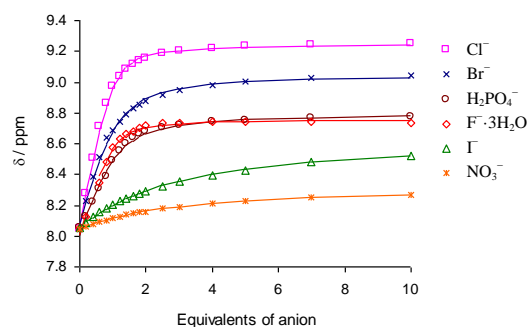
Binding Curves

Receptor 7·PF₆



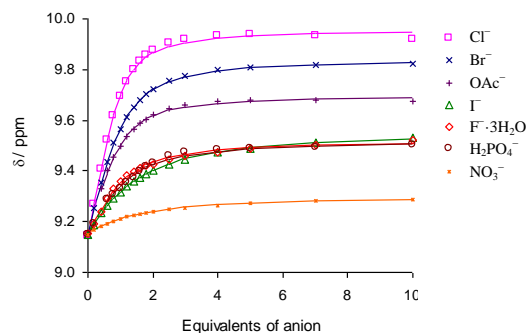
Supplementary Fig. S15 Changes in the chemical shifts of proton 10 in pyridine receptor 7·PF₆ upon addition of anions in 99:1 CD₃CN/D₂O at 293 K. Symbols represent experimental data points; lines represent calculated binding isotherms.

Receptor 8·PF₆



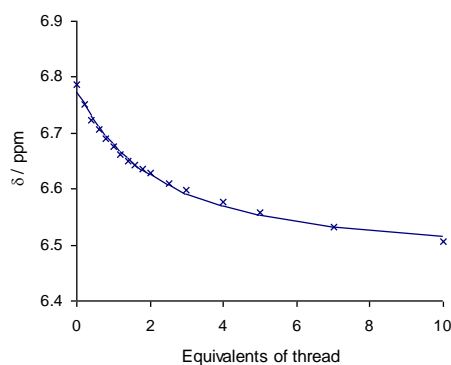
Supplementary Fig. S16 Changes in the chemical shifts of proton 10 in receptor 8·PF₆ upon addition of anions in 99:1 CD₃CN/D₂O at 293 K. Symbols represent experimental data points; lines represent calculated binding isotherms.

Receptor **9**·(PF₆)₂



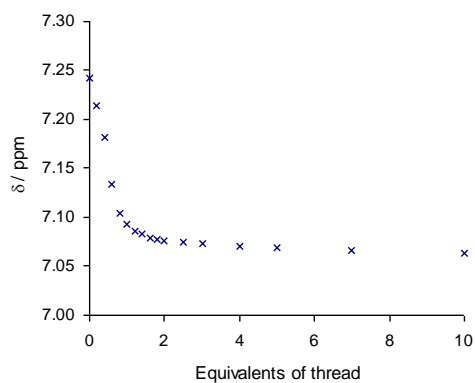
Supplementary Fig. S17 Changes in the chemical shifts of proton 10 in receptor **9**·(PF₆)₂ upon addition of anions in 95:5 CD₃CN/D₂O at 293 K. Symbols represent experimental data points; lines represent calculated binding isotherms.

Pseudorotaxane **8**·**15**·PF₆

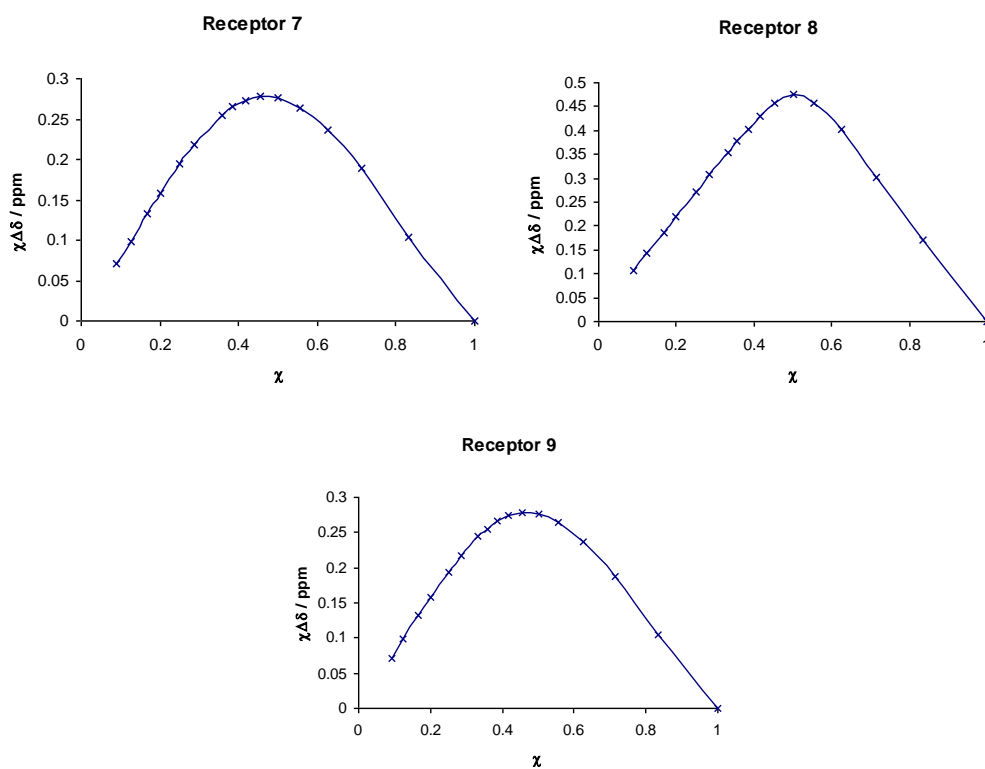


Supplementary Fig. S18 Changes in the chemical shift of hydroquinone protons (g and h) in **15** upon addition of thread **8**·PF₆ in CDCl₃ at 293K. Crosses represent experimental data points; line represents calculated binding isotherm.

Pseudorotaxane **8**·**16**·PF₆



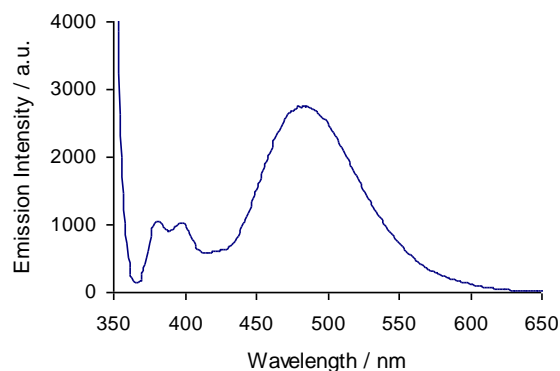
Supplementary Fig. S19 Changes in the chemical shift of phenolic protons f' in **16** upon addition of thread **8**·PF₆ in CDCl₃ at 293K.



Supplementary Fig. S20 Approximations of Job Plot experiments indicating 1:1 stoichiometries for receptors **7**·PF₆, **8**·PF₆ and **9**·(PF₆)₂ with chloride.

Part IV: Fluorescence and UV/Vis Studies

Fluorescence Spectrum



Supplementary Fig. S21 Emission spectrum of pyrene-appended receptor **14**·PF₆ in 1:1 CH₂Cl₂/acetone ($c = 5 \times 10^{-7}$ M, $\lambda_{\text{excit}} = 345$ nm, 293 K).

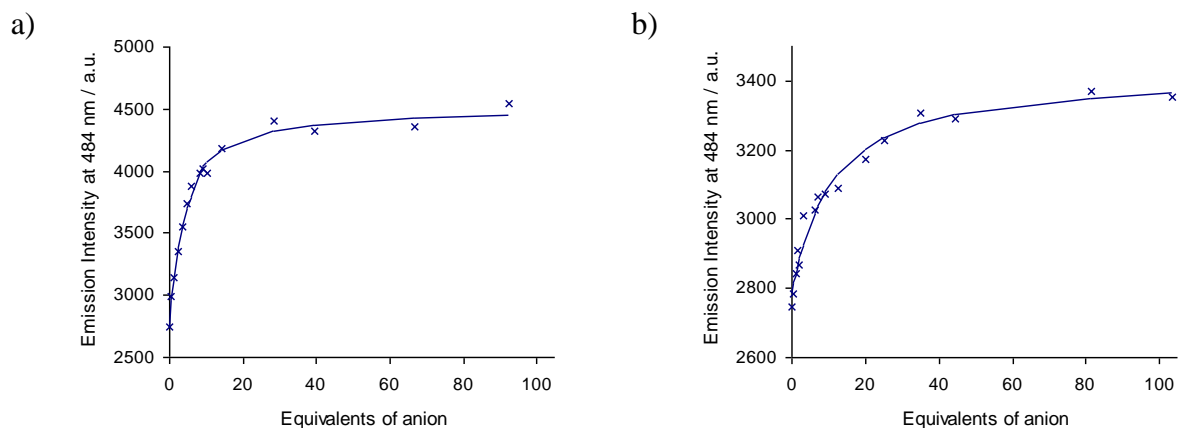
Fluorescence Protocol

Fluorescence emission spectra of **14** were recorded on Hitachi F-4500 spectrophotometer using a Hellma Quartz cuvette of pathlength 10 mm at 293 K with an excitation wavelength of 345 nm. To a 2.5 mL, 5.0×10^{-7} M solution of **14** in 1:1 CH₂Cl₂/acetone were added aliquots of the guest dissolved in a stock solution made up with the receptor, such that the same concentration of the host was maintained throughout the titration experiments. Addition was carried out up to 100 equivalents of the guest, which corresponded to approximately 0.20 mL. Excitation spectra were recorded during these titrations by monitoring both the monomer and excimer emission bands (381 and 484 nm). Where possible, the titration data were analysed using SPECFIT³ computer programme to determine log K values. The parameters were refined using a non-linear least-squares method.

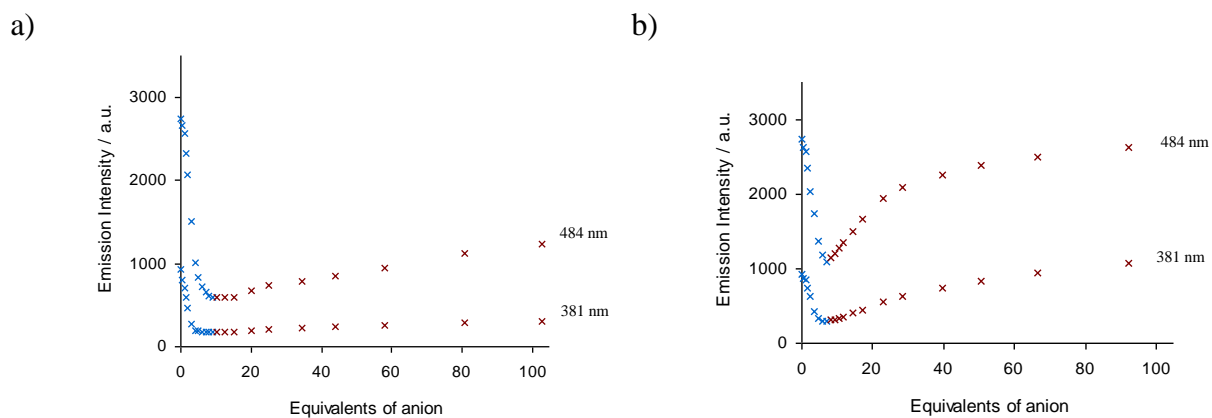
UV/Vis Protocol

The electronic absorption spectrum was recorded on a PGT60 U spectrophotometer using a Hellma Quartz cuvette of pathlength 10 mm at 293 K. To a 2.5 mL, 1.0×10^{-5} M solution of the host in 1:1 CH₂Cl₂/acetone were added aliquots of the guests corresponding to approximately 5.0 equivalents, such that 100 μ L was added and the concentration of the host remained constant.

Binding Curves

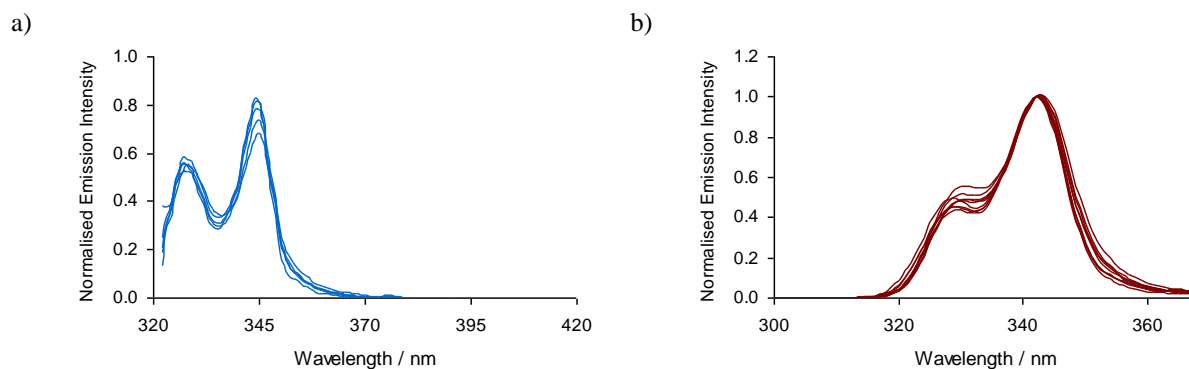


Supplementary Fig. S22 Changes in the emission intensity of pyrene-appended receptor **14**·PF₆ in 1:1 CH₂Cl₂/acetone ($c = 5 \times 10^{-7}$ M, $\lambda_{\text{excit}} = 345$ nm, 293 K) at 484 nm upon addition of a) TBACl, and b) TBABr. Symbols represent experimental data points, lines represent calculated binding isotherms. Note: different y-axis scales.



Supplementary Fig. S23 Changes in the emission intensity at 381 and 484 nm of pyrene-appended receptor **100**·PF₆ in 1:1 CH₂Cl₂/acetone ($c = 5 \times 10^{-7}$ M, $\lambda_{\text{excit}} = 345$ nm, 293 K) upon addition of a) TBAF·3H₂O, and b) TBAH₂PO₄. Blue and red represent different stages of fluorescence behaviour.

UV/Vis and Excitation Spectra



Supplementary Fig. S24 Changes in a) the UV/Vis spectrum of pyrene-appended receptor **100**·PF₆ in 1:1 CH₂Cl₂/acetone ($c = 1 \times 10^{-5}$ M), and b) the excitation spectrum of pyrene-appended receptor **14**·PF₆ in 1:1 CH₂Cl₂/acetone ($c = 5 \times 10^{-7}$ M, $\lambda_{\text{emission}} = 381$ or 484 nm), upon addition of anions at 293 K. Note: wavelengths lower than 322 nm were not possible in the UV/Vis spectrum due to the presence of acetone in the solvent mixture. Extinction coefficient of **14**·PF₆, ϵ , = 8.3×10^4 M⁻¹cm⁻¹.

Part V: References

1. M. J. Hynes, *J. Chem. Soc., Dalton Trans.*, 1993, 311-312.
2. M. T. Blanda, J. H. Horner and M. Newcomb, *J. Org. Chem.*, 1989, **54**, 4626-4636.
3. SPECFIT v.2.02, Spectrum Software Associates, Chapel Hill, NC.
4. M. J. Barrell, D. A. Leigh, P. J. Lusby and A. M. Z. Slawin, *Angew. Chem. Int. Ed.*, 2008, **47**, 8036-8039.